Prevention of Chemotherapy-Induced Alopecia in Rats by CDK Inhibitors

Stephen T. Davis,[1]* Bill G. Benson,[2] H. Neal Bramson,[3] Dennis E. Chapman,[4]† Scott H. Dickerson,[5] Karen M. Dold,[1] Derek J. Eberwein,[1] Mark Edelstein,[1] Stephen V. Frye,[5] Robert T. Gampe Jr.,[6] Robert J. Griffin,[4] Philip A. Harris,[5] Anne M. Hassell,[6] William D. Holmes,[7] Robert N. Hunter,[5] Victoria B. Knick,[1] Karen Lackey,[5] Brett Lovejoy,[6]‡ Michael J. Luzzio,[5]§ Doris Murray,[1] Patricia Parker,[1] Warren J. Rocque,[7] Lisa Shewchuk,[6] James M. Veal,[6] Duncan H. Walker,[1]‖ Lee F. Kuyper[6]

Most traditional cytotoxic anticancer agents ablate the rapidly dividing epithelium of the hair follicle and induce alopecia (hair loss). Inhibition of cyclin-dependent kinase 2 (CDK2), a positive regulator of eukaryotic cell cycle progression, may represent a therapeutic strategy for prevention of chemotherapy-induced alopecia (CIA) by arresting the cell cycle and reducing the sensitivity of the epithelium to many cell cycle–active antitumor agents. Potent small-molecule inhibitors of CDK2 were developed using structure-based methods. Topical application of these compounds in a neonatal rat model of CIA reduced hair loss at the site of application in 33 to 50% of the animals. Thus, inhibition of CDK2 represents a potentially useful approach for the prevention of CIA in cancer patients.

Chemotherapy-induced alopecia (CIA) is a frequent and emotionally distressing side effect of cancer chemotherapy (*1, 2*) for which there is currently no effective preventive therapy (*3, 4*). CIA is thought to arise when anticancer drugs ablate the proliferating epithelium and block normal maturation of precursor epithelial cells to the final hair strand product (*5*).

The sensitivity of hair follicle cells to anticancer agents is related to their state of proliferation. Many anticancer agents that cause CIA target specific phases of the cell cycle and are therefore selectively toxic to cells undergoing division (*6*). Inhibition of cell cycle progression has been shown to decrease the cytotoxic activity of cell cycle–active cytotoxic drugs (*7*). CDK2, a member of the protein kinase family that orchestrates the orderly progression of the eukaryotic cell cycle (*8*), plays a key role from late G_1 to late G_2 (*9*). We postulated that inhibition of CDK2 might provide the required control over cell division in the hair follicle to prevent CIA.

Here, we describe a class of synthetic CDK inhibitors, represented by structure **1** (Fig. 1A), which inhibit the enzyme by competing with adenosine triphosphate (ATP). As part of an ongoing effort to identify selective kinase inhibitors, we examined analogs of the 3-(benzylidene)indolin-2-ones **2**. These compounds inhibit receptor tyrosine kinases, such as epidermal growth factor receptor and Her-2 receptor kinases (*10*). Compound **3**, prepared as a homolog of compound **2**, was found to selectively inhibit CDK2 (median inhibitory concentration IC_{50} = 60 nM) and served as the lead compound for the work described here.

Structure-based methods were used to design analogs of compound **3**. CDK2 and its complexes with ATP (*11*), cyclin A (*12*), and small-molecule inhibitors (*13*) have been studied extensively by x-ray crystallography. To evaluate and select potential analogs of compound **3**, we determined the crystal structure of **3** bound to CDK2 (Fig. 1B) (*14*).

Analysis of the CDK2–compound **3** structure provided the basis for analog design. For example, position 5 of the inhibitor is adjacent to the amino group of Lys^{33}, which suggests that hydrogen bond acceptors at that position might enhance affinity for the enzyme. Similarly, lipophilic substituents at position 4 would be expected to contribute to binding through interactions with nearby hydrophobic residues such as Val^{18}. In addition, the orientation of the sulfonamide functionality at the opening to the binding cleft suggested that substituents on the sulfonamide might have minimal interaction with the protein. This knowledge can be exploited to alter other compound properties, such as pharmacokinetic and solubility characteristics, without negatively affecting enzyme binding.

Compound **4**, designed according to the above approach, was a potent and selective inhibitor of CDK2 (IC_{50} = 10 nM), a weaker inhibitor of CDK1 and CDK4 (IC_{50} = 110 and 130 nM, respectively), and a significantly weaker inhibitor of 12 other diverse protein kinases (average IC_{50} = 2 μM). A crystal structure of compound **4** in complex with CDK2–cyclin A confirmed the inhibitor binding mode and the expected interactions between protein and ligand (Fig. 1C).

The effects of compound **4** and related analogs on cell cycle progression were initially evaluated in a cell-based assay that assessed the ability of the compound to block progress from late G_1 into S phase of the cell cycle. Treatment of synchronized human diploid fibroblast (HDF) cells with compound **4** caused a reduction in bromodeoxyuridine (BrdU) incorporation into cellular DNA (IC_{50} = 2.5 μM). Flow cytometric analysis of asynchronous HDF cells was used to measure cell cycle progression, DNA synthesis, and apoptosis (*15*). Compound **4** (7.5 μM) exposure did not change the percentage of cells in G_1 and G_2-M phases of the cell cycle (Fig. 2A). However, compound **4** blocked S phase progression, as shown by the reduced amount of BrdU per cell and by the decreased percentage of BrdU-positive cells at 6 hours and 24 hours (Fig. 2B). The effects on the cell cycle were reversible; cells resumed DNA synthesis upon compound withdrawal, as shown by the increased percentage of BrdU-positive cells at 2 hours and 18 hours after compound removal (Fig. 2B). Compound **4** did not increase the number of cells containing <2N DNA, a measure of apoptosis, which suggests that it did not induce apoptosis.

Compound **4** also inhibited the phosphorylation of retinoblastoma (Rb) protein, a CDK2 substrate. Rb is a key regulator of progression of cells from G_1 into S and through S phase (*16*). Hypo- and hyperphosphorylated forms of the Rb protein were visualized by Western analysis. Treatment of HDFs with compound **4** changed the status of Rb from the hyper- to hypophosphorylated state at 6 hours and 24 hours (*15*), and the reduction of Rb phosphorylation correlated with cell cycle arrest. In addition, cyclin A protein, whose expression is required for S phase and is positively controlled

[1]Department of Cancer Biology, [2]Department of Discovery Genetics, [3]Department of Molecular Biochemistry, [4]Department of Biomet Research Support, [5]Department of Medicinal Chemistry, [6]Department of Structural Chemistry, [7]Department of Molecular Sciences, Glaxo Wellcome Research and Development, 5 Moore Drive, Research Triangle Park, NC 27709, USA.

*To whom correspondence should be addressed. E-mail: std41085@glaxowellcome.com

†Present address: Neurocrine Biosciences, 10555 Science Center Drive, San Diego, CA 92121, USA.

‡Present address: Pennie & Edmonds LLP, 3300 Hillview Avenue, Palo Alto, CA 94304, USA.

§Present address: Pfizer Inc., Pfizer Central Research, Eastern Point Road, Groton, CT 06340, USA.

‖Present address: Hoffman–La Roche Inc., 340 Kingsland Street, Nutley, NJ 07110, USA.

by CDK2–cyclin E catalytic activity, was down-regulated after compound treatment (*15, 17*). A similar reduction in cyclin A mRNA levels was observed. Compound **4** treatment did not change the protein levels of either CDK2 or cyclin E (*15, 18*). These data are consistent with inhibition of CDK2 catalytic activity and with the sequential order of cyclin E and cyclin A expression during cell cycle progression.

Pretreatment of HDF cells with compound **4** (10 μM) inhibited apoptosis induced by etoposide (Fig. 2C), as evidenced by the reduction in the number of cells containing <2N DNA. Similar results were observed for additional substituted oxindole compounds and for olomoucine (150 μM), a CDK2 inhibitor that is structurally distinct from the substituted oxindoles and considerably less potent against the CDK2 enzyme (IC_{50} ~7 μM) (*19*). We also studied the effect of compound **4** on cytotoxicity of a panel of clinical anticancer agents with both cell cycle–dependent [5-fluorouracil (5FU) (S), etoposide (S and G_2), and taxol (M)] and cell cycle–independent (cisplatin and doxorubicin) mechanisms of action. CCL64 mink lung epithelial cells are sensitive to a variety of anticancer agents and were used for these studies (*20*). Compound **4** (12 μM) reduced the cytotoxicity of taxol, etoposide, cisplatin, 5FU, and doxorubicin by factors of 5, 1.5, 8, 4, and 5, respectively (Fig. 2D). Thus, compound **4** effectively protected cells from a panel of cytotoxic agents that have diverse mechanisms of action. These data suggest that compound **4** may exert its pharmacological effects through an antiapoptotic mechanism, as has been shown previously for CDK2 inhibition (*21*). However, we cannot exclude the possibility that inhibition of additional CDKs (CDK1 and CDK4) may play a key role in the cytoprotective effects observed.

An animal model of human hair growth was used to test whether the epithelium of the hair follicle was sensitive to growth arrest by CDK2 inhibitor (*15, 22*). In this model, fresh human scalp samples are transplanted onto the skin of severe combined immunodeficient (SCID) mice (Fig. 3A). Topical treatment with compound **4** formulated in dimethyl sulfoxide (DMSO) reduced the BrdU-positive nuclear labeling index by a factor of 3 at 6 hours after treatment (Fig. 3B). The antiproliferative effect was reversible; the fraction of S-phase cells returned to control values 18 hours after topical dosing. Bright-field microscopic analysis of a skin biopsy specimen from a compound **4**–treated animal showed a reduction in the BrdU-positive cells in the epithelium of the hair follicle (Fig. 3, C and D). A similar profile was observed in rat skin (*15*). These data illustrate that the compound reached the target cell population in the hair follicle and produced the desired inhibitory effects on cell cycle progression.

The in vivo efficacy of compound **4** was studied in a neonatal rat model of CIA (*23*). Two alopecia drug regimens were studied: etoposide and cyclophosphamide-doxorubicin. Etoposide was chosen because its mechanism of action requires DNA synthesis, it frequently causes hair loss in the clinical setting, and it induces alopecia in the neonatal rat (*24*). The cyclophosphamide-doxorubicin combination is highly alopecic and is frequently prescribed for patients with advanced metastatic breast cancer (*25*). Rat pups were treated topically on the scalp with compound **4** before receiving etoposide or cyclophosphamide-doxorubicin. In animals treated on the scalp with 2.5 to 250 μg of compound **4**, hair protection was exclusively confined to the scalp (Fig. 4). Thus, whole-body hair loss served as an internal control for the alopecia-inducing effects of etoposide. Protection of the hair was marked; compound **4** treatment protected 50% of the rats from etoposide-induced alopecia, with an additional 20% of the animals showing partial protection (Table 1).

The histopathological profile of etoposide-treated rat skin was improved by compound **4** in a number of ways. Compound **4** treatment increased the number of viable hair follicles, increased the number of dermal papilla, reduced the level of inflammation, decreased the amount of cellular damage to the epithelium, reduced the thickening of the epidermis, and decreased the number of apoptotic cells in the hair follicle matrix (*15*). Moreover, 29 structural analogs of compound **4** produced similar efficacy in this model. Compound **4** treatment prevented hair loss on the scalp in 33% of the rats in the cyclophosphamide-doxorubicin model (Table 1) (*15*).

The lack of toxicity of compound **4** on normal epithelium was corroborated by studies monitoring hair growth. Compound **4** (250 μg) applied topically did not cause alopecia in either the human hair xenograft or the neonatal rat models. In addition, histopathological analysis of hematoxylin and eosin–stained rat skin sections from compound **4**–treated animals did not reveal any abnormalities in comparison to vehicle-treat-

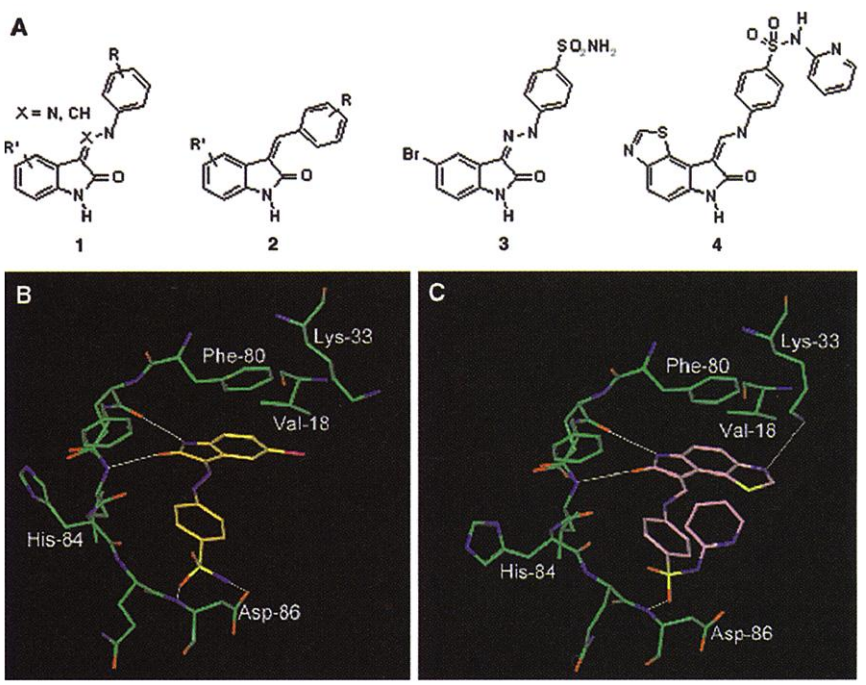

Fig. 1. (**A**) Chemical structures of compounds **1** to **4**. (**B**) X-ray crystallographic structure of CDK2 in complex with compound **3** (*15*). Atoms are color-coded as follows: protein carbon atoms, green; nitrogen, blue; oxygen, red; sulfur, yellow; and bromine, purple. The carbon atoms of compound **3** are shown in orange. The indolinone (or oxindole) moiety of compound **3** was bound at the back of the ATP site in a manner similar to that found for members of the related series **2** in complex with fibroblast growth factor (FGF) kinase (*31*). The oxindole amide group of **3** interacted with the strand of protein that connects the two domains of CDK2, donating a hydrogen bond to the backbone carbonyl of Glu^{81} and accepting a hydrogen bond from the backbone NH of Leu^{83}. The sulfonamidophenylhydrazone group projected toward the opening of the cleft, with the sulfonamide interacting with Asp^{86}. The backbone NH of Asp^{86} donated a hydrogen bond to one of the sulfonamide oxygen atoms, and the side-chain carboxyl group accepted a hydrogen bond from the sulfonamide amine function. (**C**) X-ray crystallographic structure of compound **4** bound to CDK2–cyclin A. The carbon atoms of compound **4** are shown in pink. The thiazole nitrogen atom at position 5 of compound **4** accepted a hydrogen bond from Lys^{33}, and the thiazole sulfur atom at position 4 provided hydrophobic interactions with Val^{18}. The pyridyl substituent on the sulfonamide group projected into solvent.

ed controls. Topical formulations that lack DMSO and are suitable for human testing have been developed (*26*).

The theoretical issue of antagonism of antitumor efficacy is addressed by regional delivery of the compound to the scalp and limited systemic drug exposure (*15*). Furthermore, drug combination studies of compound **4** with cytotoxic agents did not reveal evidence of tumor protection, either in colony-forming tumor survival assays in vitro or in a human colon xenograft tumor model in vivo (*15*). Finally, CDK2 inhibition may induce selective cell killing of tumor cells. Indeed, the killing of transformed cells by cell-permeable CDK2 inhibitory peptides suggests that CDK2 inhibitors have potential as antineoplastic agents (*27*).

Although CIA is considered a reversible side effect, the traumatic visual reminder and the stigma of alopecia reinforces a sense of

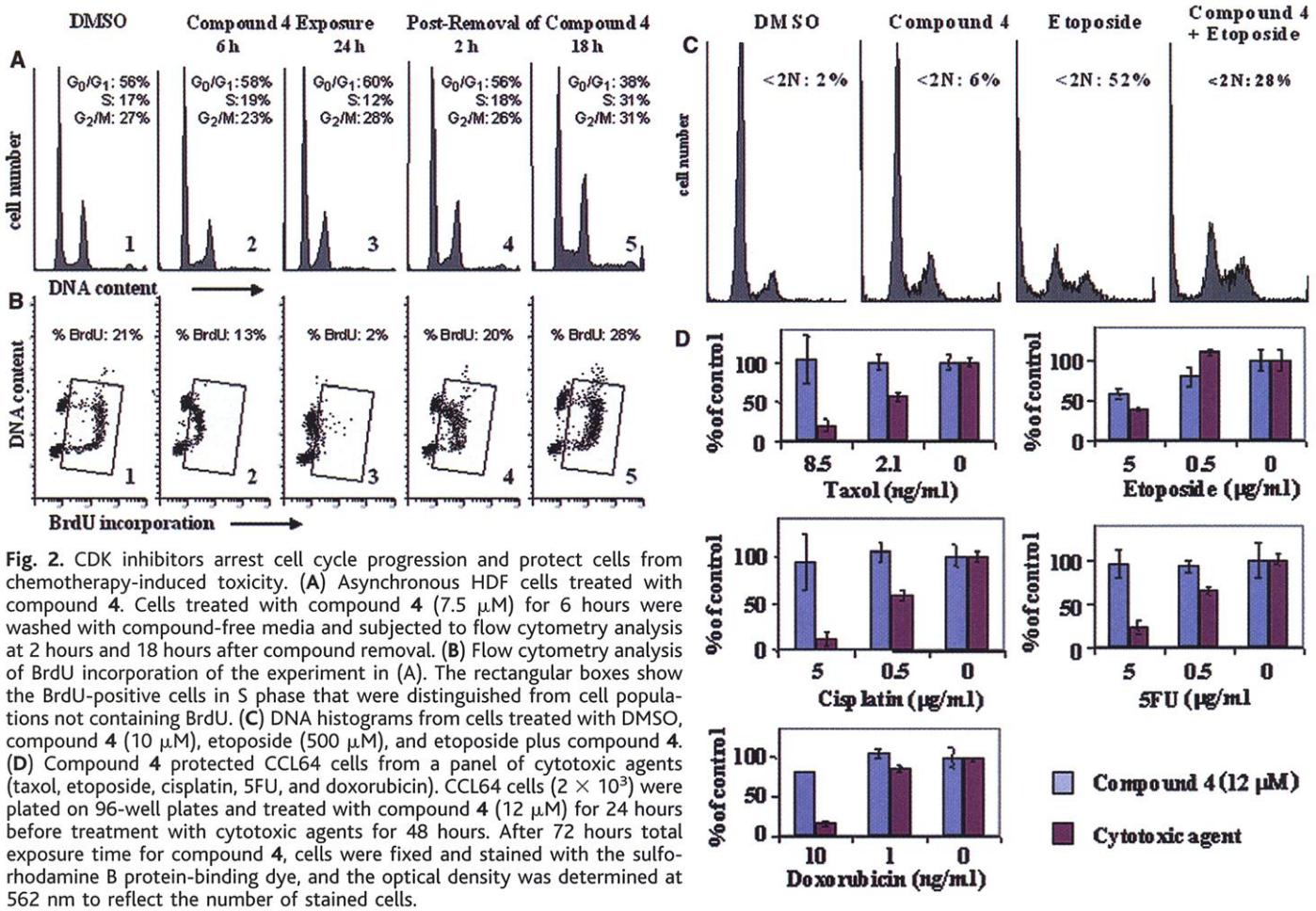

Fig. 2. CDK inhibitors arrest cell cycle progression and protect cells from chemotherapy-induced toxicity. (**A**) Asynchronous HDF cells treated with compound **4**. Cells treated with compound **4** (7.5 μM) for 6 hours were washed with compound-free media and subjected to flow cytometry analysis at 2 hours and 18 hours after compound removal. (**B**) Flow cytometry analysis of BrdU incorporation of the experiment in (A). The rectangular boxes show the BrdU-positive cells in S phase that were distinguished from cell populations not containing BrdU. (**C**) DNA histograms from cells treated with DMSO, compound **4** (10 μM), etoposide (500 μM), and etoposide plus compound **4**. (**D**) Compound **4** protected CCL64 cells from a panel of cytotoxic agents (taxol, etoposide, cisplatin, 5FU, and doxorubicin). CCL64 cells (2×10^3) were plated on 96-well plates and treated with compound **4** (12 μM) for 24 hours before treatment with cytotoxic agents for 48 hours. After 72 hours total exposure time for compound **4**, cells were fixed and stained with the sulforhodamine B protein-binding dye, and the optical density was determined at 562 nm to reflect the number of stained cells.

Table 1. Summary of compound **4** efficacy in the prevention of hair loss in the neonatal rat. The amount of hair present on rat scalp at day 21 was scored as follows: I, no hair; II, <50% hair; III, >50% hair; and IV, 100% hair. Because greater than 50% hair loss on a human scalp is required for a clearly noticeable cosmetic change, grade III and IV animals were categorized as responders, and grade II animals were categorized as partial responders. The total number of responders relative to the total number of animals studied, expressed as a percentage, was determined from nine experiments for the etoposide model and three experiments for the cyclophosphamide-doxorubicin model. Compound **4** efficacy data were analyzed by comparing percentages of drug-treated responders (III and IV) and vehicle-treated responders. A χ^2 analysis of the composite data for the drug-treated and vehicle-treated groups was used to address experiment-to-experiment variability and to assess meaningful differences. The dosing schedule of compound **4** consisted of two doses, either at 4 and 2 hours or at 10 and 4 hours before cytotoxic therapy.

Cytotoxic model	Compound **4** schedule	Drug conc. (mg/ml)	DMSO vehicle*		Compound **4***		χ^2 *P* value (drug versus vehicle responses)
			Partial responses/ total	Responses/ total	Partial responses/ total	Responses/ total	
Etoposide	$T = -4, -2$ hours	5			7/45 (15)	24/45 (53)	<0.001
	$T = -4, -2$ hours	0.5			12/53 (23)	28/53 (53)	<0.001
	$T = -4, -2$ hours	0.05			11/48 (23)	30/48 (62)	<0.001
	$T = -4, -2$ hours	0	0/53 (0)	3/53 (6)			
Cyclophosphamide-doxorubicin	$T = -10, -4$ hours	5			4/24 (17)	8/24 (33)	0.002
	$T = -10, -4$ hours	0	0/24 (0)	0/24 (0)			

*The percentage of responders relative to the total number of animals studied is indicated in parentheses.

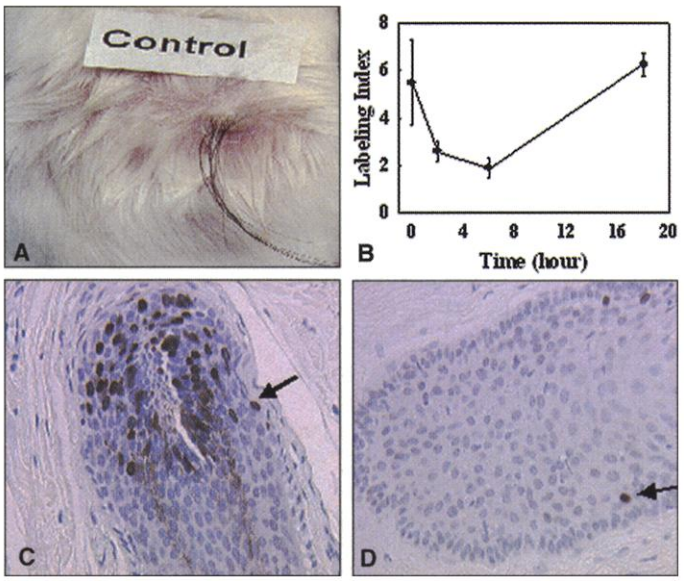

Fig. 3. Antiproliferative activity of compound **4** in follicular epithelium derived from human scalp tissue. (**A**) SCID mouse containing human scalp xenograft with actively growing hair. (**B**) Animals containing viable hair were dosed topically with compound **4** (25 μg; 50 μl of 0.5 mg/ml DMSO). Skin was removed at 2, 6, and 18 hours after compound application from animals treated with BrdU (120 mg/kg) before skin removal, and sections were immunostained using antibody to BrdU. Sections were analyzed microscopically using an Olympus Vanox-S microscope with CCD camera, interfaced with Image-pro Plus software. Nuclei from five sections per mouse, five separate high-power fields (400×) per section, and two mice per time point were counted. At least 200 nuclei were counted per field. The labeling index (LI) reflects the fraction of BrdU-positive nuclei (brown) relative to total nuclei counted, expressed as a percentage. The mean LI (%) showing standard error is plotted. (**C** and **D**) Light microscope sections of skin biopsies stained for BrdU from a DMSO-treated control animal at 6 hours (C) and a compound **4**–treated animal at 6 hours (D). Arrows indicate BrdU-positive cells.

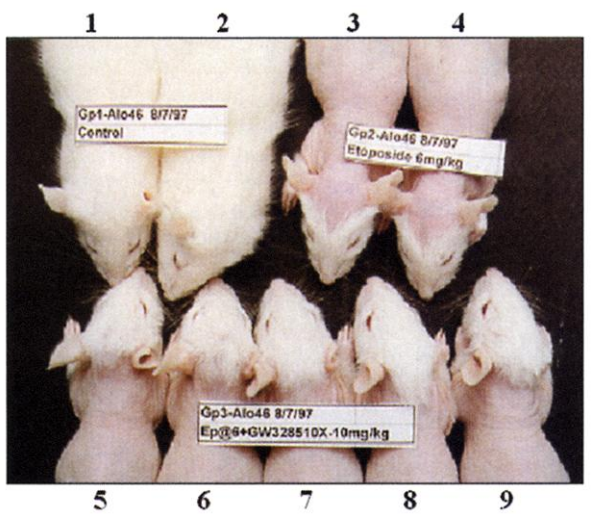

Fig. 4. Compound **4** prevents hair loss in a neonatal rat model of CIA. Rat pups (13 days of age, actively growing hair) were pretreated 4 hours and 2 hours (t = −4 and −2 hours) with topical application of compound **4** (250 μg; 50 μl of 5 mg/ml DMSO) to the scalp, then injected with etoposide. Etoposide induced total alopecia within 1 week of administration. Hair was assessed and photographed on day 21. The protective activity was schedule dependent. Two applications, 4 hours and 2 hours before etoposide, were optimal for protection. Post-treatment schedules were ineffective in preventing hair loss. Shown are two animals from the untreated group (– etoposide, upper left panel, animals 1 and 2); two animals from DMSO-treated group (+ etoposide, upper right, animals 3 and 4), and five animals from compound **4**–treated group (+ etoposide, lower panel, animals 5 to 9). Experiments were repeated at least nine times with five rats per experimental subgroup.

helplessness and the perception that the patient may not survive his or her disease. On the basis of the evidence presented here, clinical trials in cancer patients to assess the efficacy of this approach to prevent CIA may be warranted.

References and Notes

1. V. J. Dorr, *Semin. Oncol.* **25**, 562 (1998).
2. K. Munstedt, N. Manthey, S. Sachsse, H. Vahrson, *Support. Care Cancer* **5**, 139 (1997).
3. G. Chen *et al.*, *Int. J. Cancer* **75**, 303 (1998).
4. M. Duvic *et al.*, *J. Am. Acad. Dermatol.* **35**, 74 (1996).
5. R. Paus, G. Cotsarelis, *N. Engl. J. Med.* **341**, 491 (1999).
6. Z. Darzynkiewicz, *J. Cell. Biochem.* **58**, 151 (1995).
7. S. Bruno, B. Ardelt, S. J. Skierski, F. Traganos, Z. Darzynkiewicz, *Cancer Res.* **52**, 470 (1992).
8. M. Ohtsubo, A. M. Theodoras, J. Schumacher, J. M. Roberts, M. Pagano, *Mol. Cell. Biol.* **15**, 2612 (1995).
9. S. van den Heuvel, E. Harlow, *Science* **262**, 2050 (1993).
10. L. Sun *et al.*, *J. Med. Chem.* **41**, 2588 (1998).
11. U. Schulze-Gahmen, H. L. De Bondt, S.-H. Kim, *J. Med. Chem.* **39**, 4540 (1996).
12. A. A. Russo, P. D. Jeffrey, N. Pavletich, *Nature Struct. Biol.* **3**, 696 (1996).
13. S.-H. Kim, *Pure Appl. Chem.* **70**, 555 (1998).
14. CDK2 was expressed, purified, and crystallized as described (*28*). Crystals were soaked with 1 mM compound **3** for 3 to 7 days. Data were collected [2.2 Å resolution (reflections/observations, 13,372/157,652; R_{merge}, 7.6%)] at room temperature on an RAXISII area detector using a Rigaku rotating anode generator and was processed and scaled with DENZO and SCALEPACK (*29*). The structure was solved by molecular replacement using CNS (*30*) and coordinates 1HCL from the Protein Data Bank. The inhibitor was fitted with QUANTA and the entire structure refined with CNS. The structure was refined to an R factor of 19% at 2.2 Å resolution with root mean square (RMS) bonds and angles equal to 0.009 Å and 1.33°, respectively. CDK2–cyclin A crystals were cross-linked with 25% glutaraldehyde for 15 min, then soaked with 1 mM compound **4** for 3 to 7 days. Before data collection, glycerol was added to 25% and the crystals were flash-frozen in liquid nitrogen. Data were collected at the IMCA beam, sector 17, at Argonne National Laboratory on a MAR charge-coupled device (CCD) detector. Data were collected to 2.8 Å resolution (reflections/observations, 53,347/541,713; R_{merge}, 7.0%) and were processed and scaled with HKL2000. The structure was solved by molecular replacement using CNS and coordinates 1FIN from the Protein Data Bank. The inhibitor was fitted with QUANTA and the entire structure refined with CNS. The structure was refined to an R factor of 21% at 2.8 Å resolution with RMS bonds and angles equal to 0.009 Å, 1.39° respectively.
15. See www.sciencemag.org/cgi/content/full/291/5501/134/DC1 for supplementary data and analytical methods.
16. R. A. Weinberg, *Cell* **81**, 323 (1995).
17. K. Zerfass-Thome *et al.*, *Mol. Cell. Biol.* **17**, 407 (1997).
18. K. M. Dold, unpublished data.
19. C. Buquet-Fagot, F. Lallemand, M.-N. Montagne, J. Mester, *Anti-Cancer Drugs* **8**, 623 (1997).
20. E. S. McCormack *et al.*, *Biochem. Pharmacol.* **53**, 1149 (1997).
21. B. Levkau *et al.*, *Mol. Cell* **1**, 553 (1998).
22. D. Lobe, S. T. Davis, in preparation.
23. Because there are currently no effective therapies for human CIA, there are no validated animal models that predict drug efficacy in human CIA. Other drug candidates, such as the vitamin D_3 analog calcitriol, have shown activity in the neonatal rat model of CIA but have not prevented CIA in humans [M. Hidalgo *et al.*, *Anti-Cancer Drugs* **10**, 393 (1999)]. This may be due to differences between rodent and human hair follicle biology [J. P. Sundberg, L. E. King, *Dermatol. Clin.* **14**, 619 (1996)].
24. J. J. Jimenez, A. A. Yunis, *Cancer Res.* **52**, 5123 (1992).
25. J. Harris, M. Morrow, G. Bonadonna, in *Cancer: Principles and Practice of Oncology*, V. T. DeVita, S. Hellman, S. A. Rosenberg, Eds. (Lippincott, Philadelphia, ed. 4, 1993), pp. 1264–1332.
26. S. Mehta, S. Williams, unpublished data.
27. Y.-n. P. Chen *et al.*, *Proc. Natl. Acad. Sci. U.S.A.* **96**, 4325 (1999).
28. L. Shewchuk *et al.*, *J. Med. Chem.* **43**, 133 (2000).
29. Z. Otwinowski, W. Minor, *Methods Enzymol.* **276**, 307 (1997).
30. A. T. Brünger *et al.*, *Acta Crystallogr.* **D54**, 905 (1998).
31. M. Mohammadi *et al.*, *Science* **276**, 955 (1997).

32. We thank E. Paul for her leadership and contributions to this project; S. Mehta, S. Williams, and M. Sacchetti for pharmaceutics support; and D. Lobe for his insight with the human hair model. The use of the beamline 17-ID in the facilities of the Industrial Macromolecular Crystallography Association Collaborative Access Team (IMCA-CAT) at the Advanced Photon Source was supported by the U.S. Department of Energy, Basic Energy Sciences, Office of Science, under contract W-31-109-Eng-38. Protein coordinates are available from the Protein Data Bank (CDK2–compound **3**, 1fvt; CDK2–cyclin A–compound **4**, 1fvv).

7 August 2000; accepted 22 November 2000